

Optimization of Transversal Relaxation of Nitroxides for Pulsed Electron–Electron Double Resonance Spectroscopy in Phospholipid Membranes

Reza Dastvan,[†] Bela E. Bode,^{†,‡} Muruga Poopathi Raja Karupppiah,^{§,||} Andriy Marko,[†] Sevdalina Lyubenova,[†] Harald Schwalbe,[§] and Thomas F. Prisner^{*,†}

Institute of Physical and Theoretical Chemistry, Institute of Organic Chemistry and Chemical Biology, and Center for Biomolecular Magnetic Resonance, Goethe University, Max-von-Laue-Strasse 7, 60438 Frankfurt am Main, Germany

Received: June 29, 2010; Revised Manuscript Received: August 31, 2010

Pulsed electron–electron double resonance (PELDOR) spectroscopy is increasingly applied to spin-labeled membrane proteins. However, after reconstitution into liposomes, spin labels often exhibit a much faster transversal relaxation (T_m) than in detergent micelles, thus limiting application of the method in lipid bilayers. In this study, the main reasons for enhanced transversal relaxation in phospholipid membranes were investigated systematically by use of spin-labeled derivatives of stearic acid and phosphatidylcholine as well as spin-labeled derivatives of the channel-forming peptide gramicidin A under the conditions typically employed for PELDOR distance measurements. Our results clearly show that dephasing due to instantaneous diffusion that depends on dipolar interaction among electron spins is an important contributor to the fast echo decay in cases of high local concentrations of spin labels in membranes. The main difference between spin labels in detergent micelles and membranes is their local concentration. Consequently, avoiding spin clustering and suppressing instantaneous diffusion is the key step for maximizing PELDOR sensitivity in lipid membranes. Even though proton spin diffusion is an important relaxation mechanism, only in samples of low local concentrations does deuteration of acyl chains and buffer significantly prolong T_m . In these cases, values of up to 7 μ s have been achieved. Furthermore, our study revealed that membrane composition and labeling position in the membrane can also affect T_m , either by promoting the segregation of spin-labeled species or by altering their exposure to matrix protons. Effects of other experimental parameters including temperature (<50 K), presence of oxygen, and cryoprotectant type are negligible under our experimental conditions.

Introduction

Although more than 30% of known genomes encode membrane proteins^{1,2} and it is estimated that over 60% of all currently available drugs target these molecules,³ determining their structure at high resolution remains a difficult challenge. Furthermore, while most membrane proteins are isolated and purified by the use of detergents, their reconstitution into liposomes is a crucial step in studying the mechanisms of action in the native environment. Reconstitution is of great significance, because many membrane proteins will display their full activity only if they are properly oriented and inserted into a lipid bilayer.^{2,4–6} The high sensitivity of electron paramagnetic resonance (EPR) spectroscopy makes it a valuable tool to study site-specific nitroxide-labeled membrane proteins in their native environments with reasonably small sample quantities.^{7,8} Pulsed electron–electron double resonance (PELDOR)^{9,10} is a powerful pulsed EPR technique to determine long-range distances^{11,12} and relative orientations^{13–15} in spin-labeled macromolecules and

thus provides valuable information and long-range restraints for structural modeling.¹⁶ However, the applicability of PELDOR to membrane proteins in reconstituted systems has been limited because of much shorter transversal relaxation time or generally spin echo dephasing time (T_m) of spin labels in lipid vesicles^{14,17–23} as compared to detergent micelles.^{14,22,24} Short T_m reduces the signal-to-noise ratio. A compensation of this effect by use of longer accumulation time or larger amount of sample is not always possible. In general, spin echo dephasing determines the feasibility of doing pulse experiments that depend upon echo detection.²⁵ Therefore, it limits the observation time window for PELDOR and thus the maximum distance that can be measured due to Fourier arguments.¹² T_m of nitroxides in detergent micelles at 50 K is on the order of a few microseconds ($\sim 2–3 \mu$ s), but in phospholipid membranes it can be less than 1 μ s.^{14,17–23} Such rapid spin echo dephasing is too fast for a reliable extraction of distances larger than 3 nm or the quantitative interpretation of broad distance distributions as commonly observed in membrane proteins.¹² In addition, the primary PELDOR data are composed of the desired specific dipolar interaction of the spin labels in the molecule or oligomer under investigation (V_{intra}) and a background contribution caused by the finite concentration of spins (intermolecular background decay, V_{inter}).^{26–28} The extraction of distances relies on a good estimate of the background function, which can be achieved only if a reasonable part of the dipolar evolution time is obtained (e.g., several times the inverse dipolar coupling). Back-

* Corresponding author: phone +49 69 798 29449; fax +49 69 798 29404; e-mail prisner@chemie.uni-frankfurt.de.

[†] Institute of Physical and Theoretical Chemistry and Center for Biomolecular Magnetic Resonance.

[‡] Present address: Leiden Institute of Chemistry, University of Leiden, Einsteinweg 55, 2333 CC Leiden, The Netherlands.

[§] Institute of Organic Chemistry and Chemical Biology and Center for Biomolecular Magnetic Resonance.

^{||} Present address: School of Chemistry, Madurai Kamaraj University, Palkalai Nagar, Madurai 625021, India.

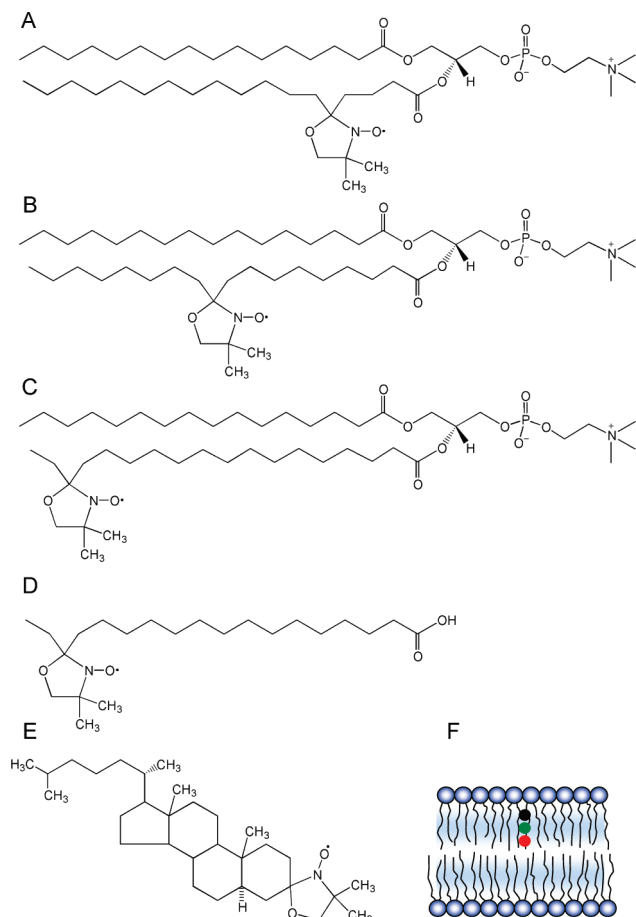


Figure 1. Chemical structure of lipid analogues used in this study: (A) 1-Palmitoyl-2-stearoyl-(5-doxy)-*sn*-glycero-3-phosphocholine (5-PCSL); (B) 1-Palmitoyl-2-stearoyl-(10-doxy)-*sn*-glycero-3-phosphocholine (10-PCSL); (C) 1-Palmitoyl-2-stearoyl-(16-doxy)-*sn*-glycero-3-phosphocholine (16-PCSL); (D) (16-doxy)-stearic acid (16-SASL); (E) (3 β -doxy)-5 α -cholestane (SL-chol); (F) average position of *n*-PCSLs in bilayer membranes.

ground correction of time traces with low signal-to-noise ratio, a short time window, or fast-decaying background is complicated and uncertain.¹² Therefore, it seems that the fast relaxation rates of spin-labeled membrane proteins in lipid bilayers are the major challenge for PELDOR applicability to such systems. Although in several recent publications some methods are implemented to optimize sample conditions for PELDOR on spin-labeled membrane-associated proteins,^{14,20,29–31} to our best knowledge, the present work is the first systematic study of the mechanisms that are involved in enhanced transversal relaxation of nitroxides in phospholipid membranes. In order to optimize samples for PELDOR with respect to T_m , we studied the Hahn echo decay of spin labels in phospholipid vesicles under the conditions typically employed for PELDOR. The doxyl (4,4-dimethylxazolidine-*N*-oxyl) derivatives of stearic acid^{32–36} and phosphatidylcholine^{37–41} (Figure 1) utilized in this study are well-established spin label model systems for EPR studies in lipid membranes. In addition, C-terminal spin-labeled gramicidin A (gA-PROXYL), as an extensively studied membrane-embedded peptide forming head-to-head dimers,^{42,43} has been utilized to compare its relaxation behavior with that of the spin-labeled lipids in order to evaluate the optimization procedure on a membrane-embedded peptide.

T_m can be measured in a two-pulse Hahn echo experiment. When the time between the two pulses (τ) is increased, the echo is usually found to decay exponentially. Any process that shifts

the resonance frequency of the electron spin by $1/\tau$ or more will prevent the spin from refocusing to form the echo, and such a process constitutes a dephasing mechanism.²⁵ These processes can be electron–electron dipole–dipole interaction,^{44,45} nuclear spin diffusion,^{25,44,46,47} instantaneous diffusion,⁴⁴ intramolecular dynamic processes, and processes that average magnetically inequivalent environments, such as librational motions,²⁵ rotation of methyl groups to which the unpaired electron is coupled,⁴⁶ and relaxation of spin-coupled systems.²⁵ Furthermore, longitudinal relaxation (T_1) poses an upper limit to T_m .⁴⁴ All of these processes can contribute to T_m in solids and frozen solutions. We performed two-pulse Hahn echo and four-pulse PELDOR experiments to investigate how different factors—including local and total spin label concentration, matrix deuteration, measurement temperature, presence of oxygen as paramagnetic relaxing agent, membrane composition and labeling position in the membrane, and cryoprotectant type—affect the transversal electron spin relaxation.

Materials and Methods

Materials. 1,2-Dipalmitoyl-*sn*-glycero-3-phosphocholine (DPPC), 1,2-dipalmitoyl(d_{62})-*sn*-glycero-3-phosphocholine (DPPC- d_{62} ; 12.55 mM in chloroform), 1-palmitoyl-2-oleoyl-*sn*-glycero-3-phosphocholine (POPC), 1,2-dioleoyl-*sn*-glycero-3-phosphocholine (DOPC), 1-palmitoyl-2-oleoyl-*sn*-glycero-3-phosphocholine (1'-*rac*-glycerol) (POPG), 1,2-dimyristoyl-*sn*-glycero-3-phosphocholine (DMPC), 1,2-dimyristoyl(d_{54})-*sn*-glycero-3-phosphocholine-1,1,2,2- d_4 -*N,N,N*-trimethyl- d_9 (DMPC- d_{67}), cholesterol, and 1-palmitoyl-2-stearoyl-(*n*-doxyl)-*sn*-glycero-3-phosphocholine (*n*-PCSL; 1.16 mM in chloroform) spin labels were purchased from Avanti Polar Lipids Inc. and used as received. D₂O (99.9% D), ethylene glycol- d_6 (EG- d_6 ; 99% D), CDCl₃ (99.9% D), CD₃OD (99.8% D), TFE- d_3 (99.8% D), and glycerol- d_8 (99.8% D) were from Deutero GmbH, Kastellaun, Germany. 16-Doxy-stearic acid (16-SASL), 3 β -doxy-5 α -cholestane (SL-chol), 2,2,6,6-tetramethyl-1-piperidinyloxy (TEMPO), 2,2,5,5-tetramethyl-3-pyrrolin-1-oxyl-3-carboxylic acid (3-carboxy-PROXYL) spin labels, octadecane 99%, valine, formic acid, anhydrous dimethylformamide (DMF), anhydrous ethanol, *N,N'*-dicyclohexylcarbodiimide (DCC), 4-(dimethylamino)pyridine (DMAP), sodium dodecyl sulfate, and sodium dodecyl sulfate- d_{25} (SDS- d_{25}) were purchased from Sigma–Aldrich (Germany). *n*-Dodecyl β -D-maltoside (DDM) and acetic anhydride were obtained from Fluka. 9-Fluorenylmethoxycarbonyl- (Fmoc-) amino acids, 2-(1*H*-benzotriazol-1-yl)-1,1,3,3-tetramethyluronium hexafluorophosphate (HBTU), *N,N*-diisopropylethylamine (DIPEA), and glycinol 2-chlorotriyl resin were purchased from Novabiochem (Merck, Germany). Trifluoroacetic acid (TFA) was obtained from Roth GmbH, Germany. Chlorotriisopropylsilane (95%) and analytical-grade dimethylformamide (DMF) were purchased from Acros Organics, Belgium. Pyridine, *tert*-butyl methyl ether, and HPLC-grade methanol were purchased from Merck KGaA, Germany.

Sample Preparation. Stock solutions of the phospholipids (25 mM), cholesterol (30 mM), and 16-SASL and SL-chol (13 mM) were prepared in chloroform, and for spin label solutions the concentrations have been calibrated against TEMPO by use of an Elexsys E500 9 GHz EPR spectrometer (Bruker). Samples with the desired spin label/phospholipid (SL/PL) molar ratio were transferred to a test tube, the solvent was evaporated with an argon gas stream, and residual traces were removed by drying under vacuum for at least 4 h before the vacuum was released by nitrogen. The dry lipids were dispersed in 10 mM phosphate-buffered saline (pH 7.4; Sigma) or in deuterium-exchanged

buffer (by three times freeze-drying) at a concentration of ≤ 100 mg/mL, by vortex mixing at room temperature or 60°C (for DPPC).^{35,40} In order to prepare the sample of 16-SASL in DDM micelles, a 12.8 mM solution of DDM (critical micelle concentration is 0.18 mM in 20°C) in phosphate buffer was prepared and then added to a preformed film of spin-labeled lipid. In these preparations, an identical total spin-label concentration of $\sim 100\ \mu\text{M}$ was prepared except for 16-SASL in POPC (1:1000) concentrated with a benchtop centrifuge to remove the excess supernatant. All the samples were deoxygenated by purging with argon (excluding the samples for the effect of oxygen that were purged with air) and were mixed in a glovebag (Aldrich AtmosBag) under nitrogen with 20% (v/v) deoxygenated ethylene glycol [except for 16-SASL in POPC (1:1000)] and transferred to standard 4 mm diameter quartz EPR tubes (Wilmod). The samples were shock-frozen in a mixture of methylcyclohexane/isopentane (1:4) that was immersed in liquid nitrogen.

Reconstitution of spin-labeled gA (see Supporting Information for the synthesis) into the liposome vesicles was achieved by the following general procedure, unless otherwise mentioned. The spin-labeled gramicidin peptide (gA-PROXYL) and phospholipids (DMPC or DPPC) were dissolved separately in TFE- d_3 or $\text{CDCl}_3:\text{CD}_3\text{OD}$ (3:1 v/v). The desired amounts of peptide and lipid solution were mixed from the stock to achieve the peptide/lipid molar ratio. The solvent was evaporated under argon flow to form a thin film, and excess solvent was removed by drying under vacuum overnight. The dry peptide/lipid mixture was dispersed by H_2O , D_2O , or buffer ($<200\ \mu\text{L}$) for 30 min above chain melting temperature with several vortex mixing and freeze–thaw cycles to ensure the spin-labeled peptide incorporation into the lipid membrane vesicles. The total spin concentration was kept constant in all the samples ($\sim 125\ \mu\text{M}$). The deuterated lipid samples were prepared with DMPC- d_{67} and DPPC- d_{62} in chloroform (25 mg/mL stock). The gA-PROXYL-containing large unilamellar vesicles (LUV) were achieved by use of an Avanti miniextruder with 100 nm membrane filters. The detergent-solubilized micelle samples were prepared by mixing peptide solution in TFE- d_3 into SDS micelle solution in D_2O or H_2O containing 20% glycerol or glycerol- d_8 . This solution was subjected to 30 s sonification cycles for uniform micelle formation. All the samples were deoxygenated by purging with argon, transferred to EPR tubes, and shock-frozen as mentioned above.

Pulse EPR Measurements. Pulsed EPR data were measured on an Elexsys E580 EPR spectrometer (Bruker) equipped with a Bruker PELDOR unit (E580-400U), a continuous-flow helium cryostat (CF935) and temperature control system (ITC 502), both from Oxford Instruments, at frequencies of ~ 9.6 GHz (X-band) using a standard flex line probe head housing a dielectric ring resonator (MD5 W1, Bruker). Microwave pulses were amplified by a 1 kW TWT amplifier (ASE 117x). Temperature was kept at 50 K. The shot repetition time was 1.5–3 ms, and EPR spectra were measured with field-swept, echo-detected EPR by use of a Hahn echo sequence, $2\pi/3-\tau-2\pi/3-\tau$ -echo, and a 15 mT field sweep. The pulse separation time τ was set to 200 ns for protonated samples and 380 ns for deuterated samples with a length of the $2\pi/3$ pulses of 32 ns. Transversal relaxation data were acquired with a Hahn echo sequence $\pi/2-\tau-\pi-\tau$ -echo. An initial τ of 120 ns and an increment of 4 ns were used. The integrated echo intensity was measured as a function of this increment, with an integration gate of 20–32 ns length centered at the echo maximum. The pulse lengths were 16 ns for the $\pi/2$ pulse and 32 ns for the π pulse. Instantaneous diffusion was

probed by gradually changing the flip angle of the 32 ns pulse from π to $\pi/8$.

For PELDOR experiments the dead-time free four-pulse sequence was used.¹⁰ Typical pulse lengths were 32 ns ($\pi/2$ and π) for the probe pulses and 14 ns (π) for the pump pulse. The delay between the first and second probe pulses was varied between 132 and 188 ns in 8 ns steps (for protonated samples) and between 400 and 792 ns in 56 ns steps (for deuterated samples) to reduce contributions from nuclear modulations.⁴⁸ The pulse separation between the second and third probe pulses was between 1 and 3 μs , depending on the T_m of the samples. The frequency of the pump pulse was set to center of the overcoupled resonator ($Q \sim 50$) and the magnetic field was adjusted, such that the excitation coincides with the central peak of the nitroxide powder spectrum to obtain maximum pumping efficiency. The probe frequency was chosen 70 MHz higher.

Theoretical Background. Relaxation of electron transversal magnetization observed in Hahn echo experiments arises from dipolar interaction among electron spins and the interaction of electron spins with the spins of the matrix nuclei.²⁵ Molecular motion of the spin label itself inducing relaxation can usually be neglected at temperatures of 50 K and below. Electron spin–spin interaction couples spins A (spins excited by microwave pulses) to the other electron spins, which are involved in a number of reorientation processes.⁴⁴ Depending on the system, the following electron spin reorientations can dominate: (i) inversion of one electron spin with energy exchange with the lattice, (ii) flip-flop reorientation (exchange of energy between neighboring spins with the same Zeeman energy called spin diffusion,^{25,44} and (iii) instantaneous diffusion (controlled inversion of electron spins by a microwave pulse). Very often spins B (spins not excited by microwave pulses) are involved in the first two stochastic processes that lead to spectral diffusion (SD) due to interaction of spins A with spins B. In the instantaneous diffusion process, only the electron spins excited by pulses participate.

In general, the echo intensities can be represented by a stretched exponential decay function:²⁵

$$V(2\tau) = V(0) \exp\left[-\left(\frac{2\tau}{T_m}\right)^x\right] \quad (1)$$

where $V(2\tau)$ and $V(0)$ are the echo intensity at time 2τ , twice the time between the two pulses, and echo intensity at time zero, respectively. The parameters T_m and x can be determined by fitting the experimental data (maxima of electron spin echo envelope modulation, ESEEM) with eq 1. If, for instance, nuclear spin diffusion is the main relaxation mechanism, $x \sim 2$ –2.5 is typically found.^{25,46} For processes that average inequivalent environments, such as librational motions and rotation of methyl groups, x commonly varies from ~ 2 to 0.5 as the rate of the process increases.²⁵ In many cases, the observed signal decays due to several processes though can be fitted with a simple exponential decay (eq 1; $x = 1$). Then the obtained relaxation rate $1/T_m$ can be approximately considered as a sum of all contributions mentioned above:

$$\frac{1}{T_m} \approx \frac{1}{T_{\text{ID}}^{\text{HE}}} + \frac{1}{T_{\text{SD}}} + \frac{1}{T_{\text{HF}}} \quad (2)$$

where $T_{\text{ID}}^{\text{HE}}$ and T_{SD} are the echo dephasing times associated with instantaneous and spectral diffusion, respectively. T_{HF} describes the relaxation induced by hyperfine interactions with surrounding nuclei.

The contribution of instantaneous diffusion (ID) to the Hahn echo decay in samples with homogeneous spin distribution is given by eq 3.⁴⁴

$$\frac{1}{T_{\text{ID}}^{\text{HE}}} = \frac{\pi\mu_0 g_A g_B \mu_B^2}{9\sqrt{3}\hbar} C\lambda \quad (3)$$

$$\lambda = \int \sin^2\left(\frac{\beta(\Omega_S)}{2}\right) f(\Omega_S) d\Omega_S \quad (4)$$

where μ_0 is the vacuum permeability, $g_{A,B}$ are the effective values of the \mathbf{g} -tensors of the spins, μ_B is the Bohr magneton, \hbar is the Planck constant divided by 2π , C is the concentration, Ω_S is the resonance offset, $f(\Omega_S)$ is the function describing the EPR line shape, and $\beta(\Omega_S)$ is the flip angle of the second pulse in a Hahn echo sequence in dependence of the resonance offset. By solving the Bloch equations for the longitudinal magnetization after a microwave pulse, which equals $\beta(\Omega_S)$, an expression for the integrand in eq 4 is found (eq 5) to be

$$\sin^2\left(\frac{\beta(\Omega_S)}{2}\right) = \frac{\omega_1^2}{\omega_1^2 + \Omega_S^2} \frac{1 - \cos[t_p(\omega_1^2 + \Omega_S^2)^{1/2}]}{2} \quad (5)$$

Here, ω_1 is the microwave field strength of the second pulse in angular frequencies and t_p is the pulse length.

The theoretical consideration given above allows us to analyze experimental data and estimate the contribution of each individual dephasing process to the total dephasing rate $1/T_m$. For example, performing Hahn echo experiments with different flip angles $\beta(\Omega_S)$ displays the strength of the ID contribution compared to other dephasing mechanisms. Additionally, the spatial distribution of spin labels as well as the intensity of ID, which is also proportional to the local electron spin concentration, can be probed by PELDOR. The time domain response of the PELDOR experiments is usually described as a product of two contributions (eq 6):²⁶

$$V(t) = V_{\text{intra}} V_{\text{inter}} \quad (6)$$

V_{intra} describes all spins coupled in one spin cluster, whereas V_{inter} takes into account the signal decay caused by the distribution of clusters in the sample. For the majority of spin-labeled lipids utilized in this study, spin clustering is expected to be negligible, so V_{intra} can be approximated as unity. Since PELDOR is a constant-time experiment and the intensity of the refocused echo is measured as a function of the time delay of the pump pulse, it is possible to exclusively measure instantaneous diffusion. In the PELDOR experiment, only the time during which spins evolve under a changed local dipolar field changes, whereas the contributions of all other dephasing mechanisms are constant. In case of a homogeneous distribution in three dimensions, V_{inter} can be described by eq 7:²⁷

$$V_{\text{inter}} = \exp\left(-\frac{t}{T_{\text{ID}}^{\text{PELDOR}}}\right) \quad (7)$$

$$\frac{1}{T_{\text{ID}}^{\text{PELDOR}}} = \frac{2\pi\mu_0 g_A g_B \mu_B^2}{9\sqrt{3}\hbar} C\lambda \quad (8)$$

where λ , being the fraction of spins excited by the PELDOR pump pulse at time delay t , is also determined by eq 4.

If inhomogeneous distribution of clusters occurs, characterized by a fractal dimension d , this will result in a stretched exponential decay:²⁷

$$V_{\text{inter}} = \exp(-\alpha t^{d/3}) \quad (9)$$

where parameter α describes the decay rate in this case and transforms into $1/T_{\text{ID}}^{\text{PELDOR}}$ given by eq 8 if $d = 3$.

Comparison of eqs 3 and 8 yields the following relationship for the dephasing rates caused by instantaneous diffusion in PELDOR and Hahn echo experiments:

$$\frac{1}{T_{\text{ID}}^{\text{PELDOR}}} = \frac{2\lambda_{\text{PELDOR}}}{\lambda_{\text{HE}}} \frac{1}{T_{\text{ID}}^{\text{HE}}} \quad (10)$$

where λ_{HE} is estimated to be ~ 0.3 , according to eqs 4 and 5 for a Hahn echo experiment with 32 ns inversion pulse, and λ_{PELDOR} has been determined experimentally ($\lambda_{\text{PELDOR}} \sim 0.52$).²⁸ Equation 8 can be used to determine the local concentration of spin labels in different samples from PELDOR time traces.

Results

1. Effect of Spin Label Concentration and Electron–Electron Spin Interaction. As explained in the previous section, both the local spin concentration and the spatial distribution of spin labels (16-SASL) in DPPC multilamellar vesicles can be deduced from PELDOR decay curves (Figure 2b). The curvature and slope of the PELDOR decay functions, which reflect the topology of the spin distribution and the local spin concentration via ID, respectively, differ for two samples with the same spin label (SL) but different phospholipid (PL) concentrations (molar ratios 1:100 and 1:1000). The dimensionality d of the spin label distribution function has been determined by fitting the PELDOR decay traces to eq 9. d changes from 2.3 to 2.6 for the samples with high (SL/PL 1:100) and low (SL/PL 1:1000) spin label concentration in the membrane, consistent with previous reports for spin labels in multilamellar vesicles ($2 \leq d \leq 3$).^{49,50} In addition, $T_{\text{ID}}^{\text{PELDOR}}$ changes by almost a factor of 7 by lowering the SL/PL molar ratio from 1:100 to 1:1000. If a three-dimensional distribution of spin labels is assumed, local spin concentrations of 5 mM and 700 μM can be estimated from the decays of the PELDOR time traces. These concentrations are much higher than the total sample concentration of $\sim 100 \mu\text{M}$. This difference arises from the fact that the spin labels are localized inside the lipid vesicle membranes only. Obviously, the spin labels are not randomly 3D distributed in the 1:100 sample, leading to a strongly enhanced local concentration, whereas the 1:1000 sample is closer to a statistical 3D distribution. The differences in the PELDOR trace hint at a larger average electron–electron dipolar interaction in the more concentrated sample. Moreover, the Hahn echo decay is much faster for the SL/PL 1:100 sample (Figure 2a; Table 1). The transversal relaxation time T_m increases by a factor of 1.7 from molar ratio of 1:100 to 1:1000 (Figure 2a). The estimated error of T_m measurements

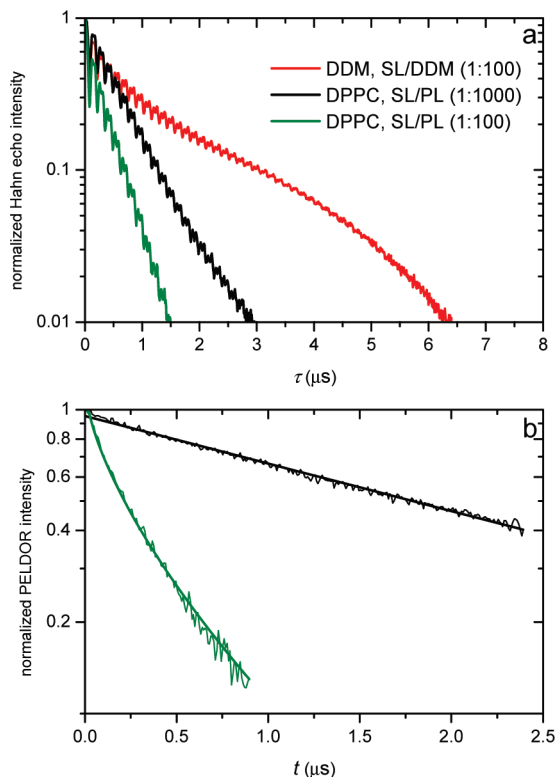


Figure 2. Effect of spin label concentration: (a) Electron spin echo decays of the 16-SASL spin label in DDM micelles and in DPPC bilayers with different spin label/phospholipid molar ratios (SL/PL). (b) PELDOR time traces of 16-SASL in DPPC bilayers and the background fits with different dimensions: SL/PL 1:100 (green, fit with $d = 2$) and SL/PL 1:1000 (black, fit with $d = 3$).

is less than 15% and is due to errors in SL/PL molar ratios and uncertainties in choosing the proper fitting curves, especially in the case of deeply modulated decay curves due to hyperfine interactions with nuclei. Further reduction of the SL/PL molar ratio ($<1:1000$) did not change T_m significantly (data not shown). Therefore, most of the further experiments were performed at a SL/PL molar ratio of 1:1000. It can be concluded that, for SL/PL molar ratios higher than 1:1000, the echo decay is dominated by intermolecular dipolar interactions. However, the observed enhancement in T_m from Hahn echo decays is smaller than that of T_{ID}^{PELDOR} for PELDOR decays. Thus, the Hahn echo decay of the sample with SL/PL molar ratio of 1:1000 is limited by dephasing mechanisms other than ID, which is not the case for PELDOR. Accordingly, in the case of high local spin concentration in the membrane (SL/PL 1:100), the contribution of ID to electron spin echo dephasing is significant, whereas dephasing is not dominated by ID for the sample with SL/PL molar ratio of 1:1000 (see Supporting Information).^{25,44} T_m of 16-SASL in DDM micelles with SL/DDM molar ratio of 1:100 is much longer than in the phospholipid sample with the same molar ratio (Figure 2a), which demonstrates that the major difference between spin labels in detergent micelles and membranes is their spatial distribution and thus their local concentration.^{22,29} In addition, in the low concentration regime T_m is virtually independent of the spatial distribution of the vesicles within the samples. Therefore, it is possible to enhance the total concentration of spin labels and thus the EPR signal intensity by sedimentation of the samples. In this case, the addition of a cryoprotectant is not needed, due to the decreased water content of the samples. Similar results as for the spin-labeled

TABLE 1: Spin Echo Dephasing Times (T_m) for Doxyl-Labeled Lipid Samples

sample properties ^a	T_m (μs)	T_{ID}^{PELDOR} (μs), best dimension fit ^b
16-SASL in DDM/H ₂ O/EG, SL/DDM 1:100	1.18 ± 0.04	
16-SASL in DPPC/H ₂ O/EG, SL/PL 1:100	0.37 ± 0.04	0.38, 2.36
16-SASL in DPPC/H ₂ O/EG, SL/PL 1:100, 5 K	0.39 ± 0.04	
16-SASL in DPPC/H ₂ O/EG	0.65 ± 0.04	2.70, 2.62
16-SASL in DPPC- <i>d</i> ₆₂ /D ₂ O/EG- <i>d</i> ₆ , SL/PL 1:100	0.78 ± 0.12	0.35, 2.14
16-SASL in DPPC- <i>d</i> ₆₂ /D ₂ O/EG- <i>d</i> ₆	4.12 ± 0.12	3.40, 2.80
16-SASL in DPPC- <i>d</i> ₆₂ /D ₂ O/EG- <i>d</i> ₆ , SL/PL 1:10 000	6.87 ± 0.12	16.53, 2.90
16-SASL in DPPC- <i>d</i> ₆₂ /D ₂ O/EG- <i>d</i> ₆ , 5 K	4.25 ± 0.12	
5-PCSL in DPPC/H ₂ O/EG	1.86 ± 0.06	
5-PCSL in DPPC/D ₂ O/EG- <i>d</i> ₆	1.95 ± 0.06	
5-PCSL in DPPC- <i>d</i> ₆₂ /H ₂ O/EG	2.05 ± 0.10	
5-PCSL in DPPC- <i>d</i> ₆₂ /D ₂ O/EG- <i>d</i> ₆	2.30 ± 0.10	2.74, 2.45
10-PCSL in DPPC/H ₂ O/EG	0.60 ± 0.04	
10-PCSL in DPPC/D ₂ O/EG- <i>d</i> ₆	0.81 ± 0.04	
10-PCSL in DPPC- <i>d</i> ₆₂ /D ₂ O/EG- <i>d</i> ₆	1.09 ± 0.12	1.63, 1.44
16-PCSL in DPPC/H ₂ O/EG	0.58 ± 0.04	
16-PCSL in DPPC/D ₂ O/EG- <i>d</i> ₆	0.50 ± 0.04	
16-PCSL in DPPC- <i>d</i> ₆₂ /H ₂ O/EG	2.58 ± 0.12	
16-PCSL in DPPC- <i>d</i> ₆₂ /D ₂ O/EG- <i>d</i> ₆	2.66 ± 0.12	2.76, 2.97
16-SASL in POPC/H ₂ O/EG	0.99 ± 0.04	2.50, 2.58
16-SASL in POPC/H ₂ O/EG, oxygenated	1.03 ± 0.04	
16-SASL in DOPC/H ₂ O/EG	1.24 ± 0.04	
16-SASL in POPG/H ₂ O/EG	1.12 ± 0.04	
SL-cholesterol in POPC/H ₂ O/EG	1.70 ± 0.04	2.05, 2.68
SL-cholesterol in POPC/Chol (80:20)/H ₂ O/EG	1.55 ± 0.04	
16-SASL in octadecane	0.76 ± 0.04	

^a SL/PL molar ratios are 1:1000 and temperature is 50 K if not mentioned otherwise. ^b T_{ID}^{PELDOR} values (in microseconds) and best background dimension fit values are estimated from PELDOR time traces.

TABLE 2: Spin Echo Dephasing Times (T_m) for gA-PROXYL Samples

sample properties ^a	T_m (μs) ^b
DMPC/D ₂ O, (1:100)	0.46 ± 0.10 (0.68)
DMPC/H ₂ O	1.90 ± 0.06
DMPC/D ₂ O	1.93 ± 0.10 (2.34)
DMPC- <i>d</i> ₆₇ /H ₂ O	2.10 ± 0.10
DMPC- <i>d</i> ₆₇ /D ₂ O	2.70 ± 0.12 (3.70)
DMPC- <i>d</i> ₆₇ /D ₂ O, LUV	2.66 ± 0.12
DMPC/D ₂ O, 1:2000	2.27 ± 0.10
DMPC/D ₂ O, 1:4000	2.47 ± 0.10 (6.00)
DPPC/H ₂ O	2.18 ± 0.06
DPPC/D ₂ O	2.33 ± 0.10
DPPC- <i>d</i> ₆₂ /H ₂ O	3.28 ± 0.10
DPPC- <i>d</i> ₆₂ /D ₂ O	3.75 ± 0.12
SDS- <i>d</i> ₂₅ /D ₂ O/glycerol- <i>d</i> ₈ , 1:100	5.92 ± 0.12
SDS/H ₂ O/glycerol	3.08 ± 0.06
SDS/D ₂ O/glycerol- <i>d</i> ₈	4.43 ± 0.12
SDS- <i>d</i> ₂₅ /D ₂ O/glycerol- <i>d</i> ₈	5.75 ± 0.12 (13.7)

^a Molar ratios are 1:1000 if not mentioned otherwise. ^b T_{ID}^{PELDOR} values (in microseconds) are estimated from PELDOR time traces.

lipid samples were obtained for the lipophilic C-terminus-labeled peptide gA-PROXYL in DMPC and DPPC bilayers and SDS micelles, in agreement with previous studies (Table 2 and Supporting Information).^{42,43} The estimated local peptide concentrations and corresponding dipolar decay time constants, probed by PELDOR measurements on gA-PROXYL samples (see Supporting Information), confirmed the dilution of noninteracting dimers of gA-PROXYL in DMPC bilayers by increasing the lipid content. In addition, for gA-PROXYL/DMPC (1:1000), the echo dephasing time

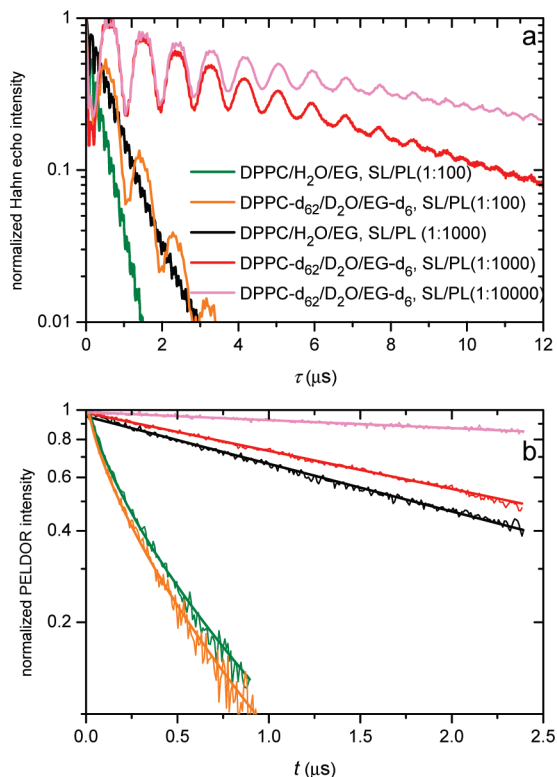


Figure 3. Effect of acyl chain and buffer deuteration: (a) Electron spin echo decays of 16-SASL in protonated and acyl chain- and buffer-deuterated DPPC bilayers with different SL/PL molar ratios. (b) PELDOR time traces of 16-SASL in protonated (green and black) and acyl chain- and buffer-deuterated (orange, red, and magenta) DPPC bilayers with SL/PL 1:100 and 1:1000(0) and 2D and 3D background fits, respectively.

T_m in large unilamellar vesicles (LUVs), in which spin labels are more uniformly distributed in the sample volume, is identical to that of multilamellar vesicles, suggesting that nitroxide spins are sufficiently separated in the later sample.

2. Effect of Acyl Chain and Buffer Deuteration. A major contribution to transversal relaxation appears in systems with abundant protons. Nuclear relaxation and nuclear motion lead to fluctuating hyperfine fields and thus to transversal relaxation of the electron spins. Therefore, we studied the influence of acyl chain and buffer deuteration on transversal relaxation of 16-SASL in DPPC membranes (Figure 3a). Since nuclear spin diffusion scales with the product of the nuclear magnetic moments of the nuclei and electron–nuclear spin–spin coupling scales with the nuclear magnetic moment, electron spin dephasing by nuclei can be roughly approximated to scale with the nuclear magnetic moment to the third power.²⁵ For the exchange of protons to deuterons, this leads to a suppression of relaxation induced by nuclei by a factor of 35 (e.g., the relative magnetic moment to the third power). For the sample with SL/PL of 1:100, it is possible to increase T_m only by a factor of 2 by acyl chain and buffer deuteration. This effect is similar to lowering the SL/PL molar ratio by an order of magnitude. However, for the sample with SL/PL of 1:1000, an enhancement of a factor of 6.4 and a T_m as long as 4.1 μ s has been achieved for the same deuteration level. For Hahn echo experiments the contribution of ID can be diminished by lowering the flip angle of the inversion pulse to $\pi/8$. T_m of the 1:100 deuterated sample increases by almost a factor of 3 in this experiment (see Supporting Information). This clearly demonstrates that, in deuterated samples, ID is the dominant dephasing mechanism

at high local concentration of spins similar to the protonated samples wherein the contribution of ID is significant. When ID is not prevalent, proton spin diffusion (mutual spin flips of neighboring protons) is the next dominant mechanism (eq 2).^{25,44,46,47} For 16-SASL in protonated DPPC membranes, the stretching exponent value, x (eq 1), is ~ 0.72 , indicating that relaxation is mainly driven by averaging nonequivalent environments such as rotation of methyl groups to which the unpaired electron is coupled.⁴⁶ This observation is in agreement with the local environment of 16-SASL in the center of phospholipid bilayers, which is exposed to aliphatic methyl groups at the end of acyl chains. Furthermore, in the case of 16-SASL, where the nitroxide radical is expected to be well embedded inside the membrane, the effect of buffer deuteration only is negligible (data not shown).

To compare the spatial distributions of spin labels, which should not be affected by matrix deuteration, we performed PELDOR measurements on the samples with deuterated matrices (Figure 3b). $T_{\text{ID}}^{\text{PELDOR}}$ values and dimensionalities of the spin label distribution are in good agreement with the protonated samples when small differences in SL/PL molar ratios due to sample preparation are considered (Table 1). It is important to note that by reducing the proton spin diffusion by deuteration, instantaneous diffusion again dominates the electron spin echo dephasing (eq 2 and Supporting Information). Therefore the molar ratio has been lowered to 1:10 000 to achieve a Hahn echo decay that is not dominated by ID and SD any more (Figure 3a and Supporting Information). The PELDOR data on the highly diluted 1:10 000 sample exhibits a homogeneous 3D distribution (best dimension fit of 2.9) and a local spin concentration of $\sim 117 \mu\text{M}$ that is in good agreement with the total sample concentration of $\sim 100 \mu\text{M}$ (Figure 3b).

3. Effect of Lipid Composition of Phospholipid Membranes. To study the effect of lipid composition on the transversal relaxation of nitroxides, samples of 16-SASL and SL-chol in protonated phosphatidylcholine bilayers with different saturation levels of acyl chains (from DPPC to DOPC) and different headgroups (POPG) have been studied (Figure 4, Table 1, and Supporting Information). The effects are more pronounced when the nature of the acyl chain is changed rather than the type of headgroup, as can be seen for 16-SASL (Table 1 and Supporting Information). From 16-SASL in DPPC to DOPC, T_m increases by a factor of 2. This enhancement might be caused by a decrease in perturbation by the nitroxide moiety in the less-ordered POPC and DOPC membranes as compared to the more ordered DPPC membranes.³⁸ However, by comparison of PELDOR time traces of DPPC and POPC samples (Figure 4b and Supporting Information), their $T_{\text{ID}}^{\text{PELDOR}}$ values are similar. Therefore, the average distance between spins is not affected and this difference in T_m might be caused by other effects such as different local concentration of protons and particularly terminal methyl groups around the spin label. Furthermore, the average lateral pressure in the middle of the bilayer is higher for DPPC in comparison to POPC and DOPC membranes as proposed by molecular dynamics simulations.⁵¹ This might increase the exposure of spin labels to chain protons.

4. Effect of Spin-Labeled Molecules and Spin Label Position. In order to investigate the dependence of the transversal relaxation of nitroxides on the immersion depths in the membranes, we utilized three different spin-labeled phosphatidylcholine analogues (*n*-PCSLs; Figure 1) in DPPC bilayers (Figure 5).^{40,52} In addition, the effect of buffer and acyl chain deuteration was studied independently and position-dependently (Figure 5, Table 1, and Supporting Information). For the buffer-

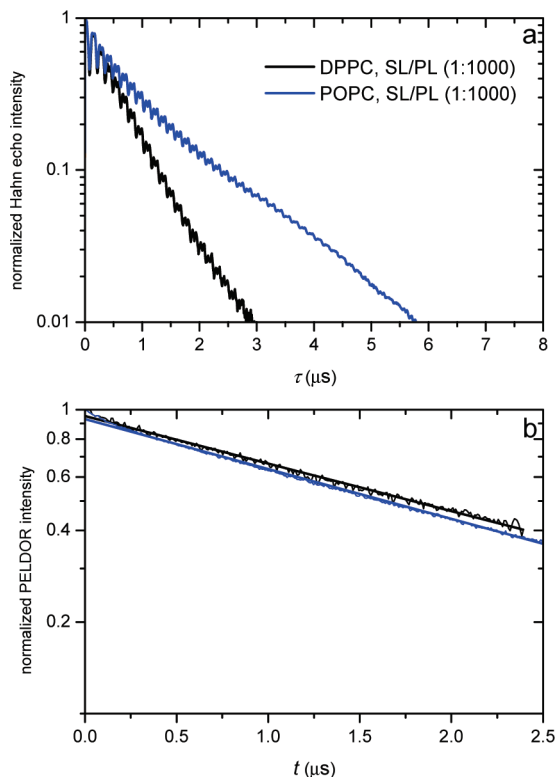


Figure 4. Effect of lipid composition: (a) Electron spin echo decays of 16-SASL in DPPC and POPC bilayers with SL/PL 1:1000. (b) PELDOR time traces of these samples and 3D background fits.

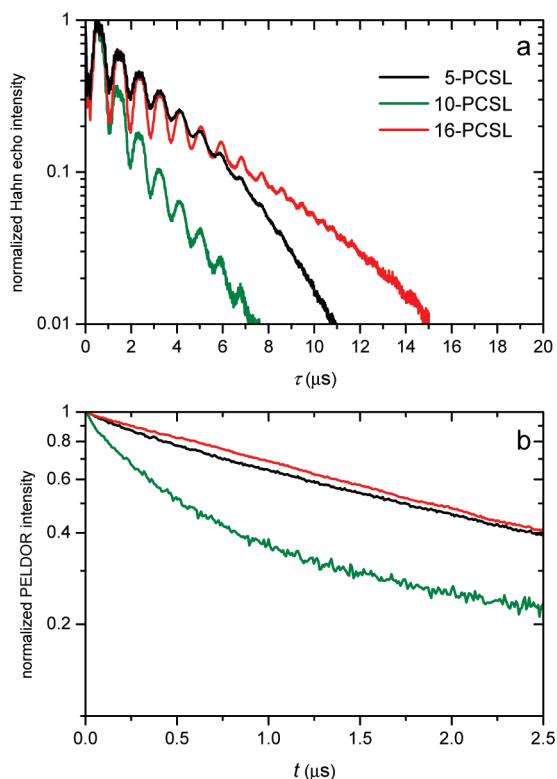


Figure 5. Effect of spin label position: (a) Electron spin echo decays of n -PCSL spin labels in acyl chain- and buffer-deuterated (DPPC- d_{62} /D₂O/EG- d_6) bilayers with SL/PL molar ratio of 1:1000. (b) PELDOR time traces of these samples.

and chain-deuterated samples, the T_m is in the order 16-PCSL > 5-PCSL > 10-PCSL (Figure 5a), whereas for protonated

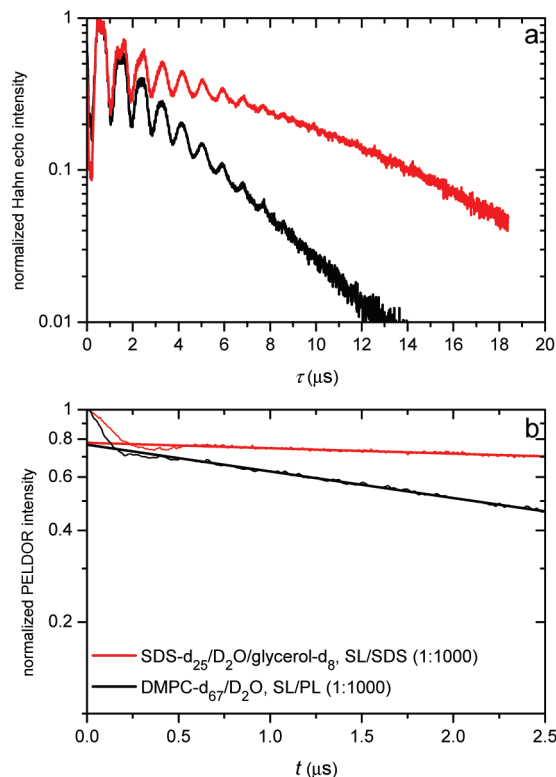


Figure 6. Comparison of the effect of matrix perdeuteration for gA-PROXYL in SDS micelles and DMPC multilamellar vesicles: (a) Electron spin echo decays; (b) PELDOR time traces.

samples, it is in the order 5-PCSL > 10-PCSL \sim 16-PCSL (Table 1 and Supporting Information). Consistent with the average position of n -PCSLs relative to the lipid–buffer interface,⁴⁰ the relaxation of 16-PCSL is independent of buffer deuteration but T_m of 5-PCSL is, by a factor of 1.1, higher in chain- and buffer-deuterated sample in comparison to just chain-deuterated sample (Table 1 and Supporting Information).

The spatial distribution of n -PCSLs in buffer- and chain-deuterated samples was investigated by PELDOR (Figure 5b). 16-PCSL showed a homogeneous three-dimensional spin distribution, whereas 5-PCSL deviates slightly and 10-PCSL deviates significantly from this behavior. Especially for 10-PCSL, this deviation can be due to segregation or clustering of spin labels,^{49,50} consistent with the shorter T_m in the perdeuterated 10-PCSL sample. In addition, our results indicate that as long as the intermolecular interactions among spin labels are comparable, electron spin echo dephasing is dependent on the immersion depth into the bilayer but independent of the nature of nitroxide spin label (see Supporting Information).

Furthermore, the effect of solvent and lipid deuteration was studied for the investigated gA-PROXYL samples (Table 2, Figure 6). In both DMPC and DPPC vesicles, the nitroxide moiety is located close to the polar–apolar interface,⁴³ and therefore the relaxation behavior of gA-PROXYL in these compositions resembles that of spin-labeled lipids such as 5-PCSL, wherein the nitroxide is in the proximity of solvent (Tables 1 and 2). In DPPC and DMPC bilayers, a significant difference in T_m can be found only between protonated and perdeuterated samples, although the T_m increment due to acyl chain deuteration is higher in DPPC compared to DMPC with the shorter acyl chain length.^{42,43} In addition, to compare spin-labeled gramicidin A in perdeuterated lipid bilayers with detergent micelles, samples of gA-PROXYL in micelles of perdeuterated SDS were prepared (Figure 6). Deuterium acces-

sibility analysis and the ^{14}N hyperfine coupling constant for gA-PROXYL in SDS micelles confirmed that nitroxides are accessible to the solvent (data not shown).⁴⁷ According to the PELDOR measurements, the overall conformation of the gramicidin dimer is conserved in SDS micelles. But in contrast to phospholipid membranes, for gA-PROXYL/SDS molar ratios lower than 1:50, echo dephasing is independent of molar ratio and T_m is significantly higher than in phospholipid membranes (Figure 6a, Table 2). Furthermore, by comparing the corresponding PELDOR traces (Figure 6b), it is clear that SDS micelles that enclose dimers are uniformly distributed in the sample ($T_{\text{ID}}^{\text{PELDOR}} \sim 13.7 \mu\text{s}$).

5. Effect of Temperature, Presence of Oxygen, and Cryoprotectant Type. T_m relaxation is well-known to be temperature-dependent. Usually the low-temperature maximum of nitroxide T_m in glassy frozen solvents is reached already at 50 K. However, if T_m is dominated by spectral diffusion, the relaxation rate will also depend on T_1 . The latter should decrease monotonously with decreasing temperature. This expectation could be confirmed by lowering the temperature to 5 K for 16-SASL in DPPC (SL/PL of 1:100). Here, the relaxation rate reduces slightly almost regardless of proticity and ID (Table 1 and Supporting Information), whereas for the concentration-optimized protonated and deuterated (DPPC) samples, T_m is independent of temperature from 50 K downward (Table 1). In the former case, T_m is dominated by spin–spin interactions, but in the latter case, nuclear spin diffusion is the dominant relaxation mechanism and at temperatures below 50 K this exhibits only small temperature dependence.⁴⁵

Oxygen is known as a paramagnetic relaxation agent for spin labels. In order to test its significance for transversal relaxation enhancement at 50 K, the concentration-optimized sample of 16-SASL in POPC was purged with air. As a result, only a small variation in T_m has been observed (Table 1). For the acyl chain- and buffer-deuterated sample of 16-SASL in DPPC- d_{62} , T_m was invariant with respect to the oxygen content, which is consistent with literature.^{25,47} In the case of DPPC multilamellar vesicles, oxygen diffusion is slow, because the membrane is already in the gel phase at room temperature. No effect has been observed for changing the cryoprotectant from ethylene glycol to glycerol and varying its concentration between 20% (v/v) and 50% (v/v). The spin labels are partitioned into the multilamellar vesicles and experience higher local concentrations as compared to the nominal bulk concentration as discussed above. Thus, aggregation of vesicles due to ice formation in the samples does not significantly alter the local concentration of spin labels. Therefore, the use of cryoprotectant at all shows little effect on T_m as compared to systems with spin labels in the aqueous phase.

Discussion

At high local concentration of spin-labeled species in the membrane, dephasing due to dipolar interaction of electron spins that manifests itself in ID due to excitation of spins by a microwave pulse is an important contributor to T_m within the studied temperature range. Thus, in the high-concentration regime, ID conceals the relaxation caused by coupling of electrons to the matrix protons of the lipid acyl chains, of the protein itself, and of the buffer (for nitroxides located in the proximity of water protons). Therefore, the first step in optimization of transversal relaxation time is to inhibit spin clustering. As for the gA-PROXYL in DMPC (Table 2 and Supporting Information), this inhibition can be achieved by increasing the ratio of lipid to spin-labeled species.^{22,29–31}

However, if spin labels tend to segregate in bilayer membranes, as in the case of 10-PCSL in DPPC membranes, then their dilution by increasing the lipid content will be less effective,^{14,17} although in such cases implementing magnetically dilute samples, in which spin-labeled membrane proteins are intermixed with wild-type proteins, is helpful.^{14,20} In the case of spin-labeled phospholipids, partial segregation of them in DPPC bilayers in the gel phase^{37–41,53} and increased segregation for labeling positions toward the center of the chain ($n = 8–10$) have been observed previously.^{37–41} These findings are in accordance with the observed order of dephasing rates 10-PCSL > 5-PCSL > 16-PCSL observed here (see Supporting Information). However, if the bilayer structure is disturbed by the nitroxide moieties and this induces segregation of labeled phospholipids, and thus enhances echo dephasing rates, then it might be possible to compensate this effect, for instance, by changing the composition of the membrane.³⁸ Lateral packing (pressure) in bilayer membranes directly depends on composition and position in the membrane. Therefore, the introduction of nitroxide spin labels leads to increased perturbation at positions where the packing level is high, for instance, close to the geometric center of the acyl chain. Accordingly, hydrophobic mismatches and lateral packing defects are important motives that stabilize the aggregate or oligomeric form of integral membrane proteins.^{42,43,54} Thus, the major parameter that governs segregation of spin-labeled species, regardless of their size and nature, might be the amount of perturbation in bilayer structure that can be introduced by inclusion of them.^{38,54}

In addition, as is evident from PELDOR data, local concentrations of 16-SASL and SL-chol in protonated DPPC and POPC membranes are similar, but the corresponding relaxation rates are significantly different (Figure 4, Table 1, and Supporting Information). For low local concentrations of spin-labeled species in membrane, transversal relaxation is mainly driven by proton spin diffusion (see Supporting Information).^{25,46,47} Generally, the transversal relaxation of electron spins below 50 K strongly depends on the concentration of nonmethyl protons and on the concentration and type of methyl protons in the environment, on length scales in the range $\sim 6–20 \text{ \AA}$.⁴⁶ Thus, a significant enhancement in T_m can be achieved by deuterium exchange of these protons.

The PELDOR background decay is governed by instantaneous diffusion. The rate of the PELDOR background decay can be related to the ID dephasing rate from the Hahn echo decay (eq 10). This is of great importance because a precise estimation of the PELDOR background function is essential for reliable extraction of distances. The contribution of ID can be separated from T_m by extrapolation to very small turning angles of the second microwave pulse (eqs 3 and 4 and Supporting Information).⁴⁴ The importance of instantaneous diffusion in echo dephasing depends on the magnitude of other contributions to T_m (eq 2).²⁵ In the case of 16-SASL in protonated DPPC membranes, ID makes an important contribution to T_m at SL/PL molar ratios of around 1:100, which corresponds to local spin concentration of a few millimolar (see Supporting Information), whereas in deuterated phospholipid membranes, the significance of ID persists to much lower spin concentrations (SL/PL molar ratio of 1:1000). In deuterated samples T_m can be enhanced maximally by a factor of 1.7 for SL/PL molar ratios lower than 1:1000 (Figure 3a). It has been shown before that at sufficiently long time, during which electron coherence evolves or at high concentrations of spin labels, the sensitivity of PELDOR can be enhanced by reducing ID via increasing the length of the observer pulses and thus decreasing the excitation

bandwidth.¹¹ In some exceptional cases, this might be an option to improve the quality of PELDOR on a given sample.

Conclusion

In this study, we systematically investigated processes that are involved in echo dephasing of nitroxide spin labels in phospholipid membranes at 50 K. In general, avoiding spin clustering and thus large instantaneous diffusion rates is the key step for the optimization of transversal relaxation of nitroxides in lipid membranes. By concentrating proteoliposomes, it is possible to recover the signal-to-noise sacrificed for low local concentrations, since T_m is virtually independent of spatial distribution of the vesicles. Only in these locally dilute samples is deuteration of lipids and buffer helpful. In addition, our study revealed that membrane composition and labeling position in the membrane can also affect T_m , either by promoting the segregation of spin-labeled species or by altering their exposure to matrix protons. Thus, if spin-labeled membrane proteins tend to segregate, then it seems that the optimization of the membrane composition, to decrease the introduced perturbation and subsequent segregation of spin-labeled species or by use of magnetically dilute samples, is inevitable. Effects of other experimental parameters including temperature (<50 K), presence of oxygen, and cryoprotectant type are negligible under our conditions. By application of similar experiments to the proxyl-labeled membrane-incorporated peptide gramicidin A, we further cross-validated the optimization procedure carried out for spin-labeled lipids and find that the optimization parameters are valid also for the membrane-embedded peptide gramicidin A. This finding further supports the usefulness of the investigation for the application to larger membrane proteins.

Acknowledgment. We acknowledge the Collaborative Research Center SFB 807 “Transport and Communication across Membranes” of the German Research Society (DFG) and the Center of Biomolecular Magnetic Resonance (BMRZ) for financial support. H.S. and T.F.P. are members of the DFG-funded Center of Excellence: Macromolecular Complexes. B.E.B. is currently supported by a Feodor-Lynen fellowship by the Alexander von Humboldt Foundation financed by the German Federal Ministry of Education and Research. M.P.R.K. is supported by the project “Phospholipid and Glycolipid Recognition, Interactions and Structures by Magnetic Resonance” (EU-PRISM). We thank Deniz Sezer for inspiring discussions and Marie Anders for technical support.

Supporting Information Available: Text and seven figures describing gA-PROXYL synthesis; dephasing by instantaneous diffusion; electron spin echo decays and corresponding PELDOR data of gA-PROXYL in DMPC with different SL/PL molar ratios; and effect of lipid composition and spin label position. This material is available free of charge via the Internet at <http://pubs.acs.org>.

References and Notes

- (1) Krogh, A.; Larsson, B.; von Heijne, G.; Sonnhammer, E. L. *J. Mol. Biol.* **2001**, *305*, 567–580.
- (2) Seddon, A. M.; Curnow, P.; Booth, P. J. *Biochim. Biophys. Acta* **2004**, *1666*, 105–117.
- (3) Overington, J. P.; Al-Lazikani, B.; Hopkins, A. L. *Nat. Rev. Drug Discovery* **2006**, *5*, 993–996.
- (4) Gustot, A.; Smriti; Ruysschaert, J. M.; Mchaourab, H.; Govaerts, C. *J. Biol. Chem.* **2010**, *285*, 14144–14151.
- (5) Aänismaa, P.; Gatlik-Landwojtowicz, E.; Seelig, A. *Biochemistry* **2008**, *47*, 10197–10207.
- (6) Rigaud, J.-L. *Braz. J. Med. Biol. Res.* **2002**, *35*, 753–766.
- (7) Perozo, E.; Cortes, D. M.; Cuello, L. G. *Nat. Struct. Biol.* **1998**, *5*, 459–469.
- (8) Hubbell, W. L.; Cafiso, D. S.; Altenbach, C. *Nat. Struct. Biol.* **2000**, *7*, 735–739.
- (9) Milov, A. D.; Salikhov, K. M.; Shirov, M. D. *Fiz. Tverd. Tela* **1981**, *23*, 975–982.
- (10) Pannier, M.; Veit, S.; Godt, A.; Jeschke, G.; Spiess, H. W. *J. Magn. Reson.* **2000**, *142*, 331–340.
- (11) Jeschke, G.; Polyhach, Y. *Phys. Chem. Chem. Phys.* **2007**, *9*, 1895–1910.
- (12) Schiemann, O.; Prisner, T. F. *Q. Rev. Biophys.* **2007**, *40*, 1–53.
- (13) Schiemann, O.; Cekan, P.; Margraf, D.; Prisner, T. F.; Sigurdsson, S. T. *Angew. Chem., Int. Ed.* **2009**, *48*, 2392–2395.
- (14) Endeward, B.; Butterwick, J. A.; MacKinnon, R.; Prisner, T. F. *J. Am. Chem. Soc.* **2009**, *131*, 15246–15250.
- (15) Marko, A.; Margraf, D.; Cekan, P.; Sigurdsson, S. T.; Schiemann, O.; Prisner, T. F. *Phys. Rev. E* **2010**, *81*, 021911.
- (16) Bhatnagar, J.; Freed, J. H.; Crane, B. R. Two-Component Signaling Systems, Part B. In *Methods in Enzymology*; Simon, M., Crane, B. R., Crane, A. B., Eds.; Academic Press: San Diego, CA, 2007; Vol. 423, pp 117–133.
- (17) Jeschke, G.; Wegener, C.; Nietschke, M.; Jung, H.; Steinhoff, H.-J. *Biophys. J.* **2004**, *86*, 2551–2557.
- (18) Hilger, D.; Jung, H.; Padan, E.; Wegener, C.; Vogel, K.-P.; Steinhoff, H.-J.; Jeschke, G. *Biophys. J.* **2005**, *89*, 1328–1338.
- (19) Hilger, D.; Polyhach, Y.; Padan, E.; Jung, H.; Jeschke, G. *Biophys. J.* **2007**, *93*, 3675–3683.
- (20) Xu, Q.; Ellena, J. F.; Kim, M.; Cafiso, D. S. *Biochemistry* **2006**, *45*, 10847–10854.
- (21) Milov, A. D.; Samoilova, R. I.; Tsvetkov, Y. D.; Formaggio, F.; Toniolo, C.; Raap, J. *J. Am. Chem. Soc.* **2007**, *129*, 9260–9261.
- (22) Zou, P.; Bortolus, M.; Mchaourab, H. S. *J. Mol. Biol.* **2009**, *393*, 586–597.
- (23) Borbat, P. P.; Surendhran, K.; Bortolus, M.; Zou, P.; Freed, J. H.; Mchaourab, H. S. *PLoS Biol.* **2007**, *5*, e271.
- (24) Upadhyay, A. K.; Borbat, P. P.; Wang, J.; Freed, J. H.; Edmondson, D. E. *Biochemistry* **2008**, *47*, 1554–1566.
- (25) Eaton, S. S.; Eaton, G. R. In *Biological Magnetic Resonance, Vol. 19, Distance Measurements in Biological Systems by EPR*; Berliner, L. J., Eaton, S. S., Eaton, G. R., Eds.; Kluwer Academics/Plenum Publishers: New York, 2000; pp 29–71.
- (26) Milov, A. D.; Ponomarev, A. B.; Tsvetkov, Y. D. *Chem. Phys. Lett.* **1984**, *110*, 67–72.
- (27) Milov, A. D.; Maryasov, A. G.; Tsvetkov, Y. D. *Appl. Magn. Reson.* **1998**, *15*, 107–143.
- (28) Bode, B. E.; Margraf, D.; Plackmeyer, J.; Dürner, G.; Prisner, T. F.; Schiemann, O. *J. Am. Chem. Soc.* **2007**, *129*, 6736–6745.
- (29) Zou, P.; Mchaourab, H. S. *Biophys. J.* **2010**, *98*, L18–20.
- (30) Hilger, D.; Polyhach, Y.; Jung, H.; Jeschke, G. *Biophys. J.* **2009**, *96*, 217–225.
- (31) Georgieva, E. R.; Ramlall, T. F.; Borbat, P. P.; Freed, J. H.; Eliezer, D. *J. Am. Chem. Soc.* **2008**, *130*, 12856–12857.
- (32) Meirovitch, E.; Nayeem, A.; Freed, J. H. *J. Phys. Chem.* **1984**, *88*, 3454–3465.
- (33) Bonosi, F.; Gabrielli, G.; Margheri, E.; Martini, G. *Langmuir* **1990**, *6*, 1769–1773.
- (34) Bratt, J. P.; Kevan, L. *J. Phys. Chem.* **1993**, *97*, 7371–7374.
- (35) Lee, D. K.; Kim, J. S.; Lee, Y. M.; Kang, Y. S.; Kim, B. K. *Langmuir* **1998**, *14*, 5184–5187.
- (36) Isaev, N. P.; Dzuba, S. A. *J. Phys. Chem. B* **2008**, *112*, 13285–13291.
- (37) Fajer, P.; Watts, A.; Marsh, D. *Biophys. J.* **1992**, *61*, 879–891.
- (38) Earle, K. A.; Moscicki, J. K.; Ge, M.; Budil, D. E.; Freed, J. H. *Biophys. J.* **1994**, *66*, 1213–1221.
- (39) Dzikovski, B. G.; Livshits, V. A.; Marsh, D. *Biophys. J.* **2003**, *85*, 1005–1012.
- (40) Bartucci, R.; Guzzi, R.; Marsh, D.; Sportelli, L. *Biophys. J.* **2003**, *84*, 1025–1030.
- (41) Bartucci, R.; Guzzi, R.; Marsh, D.; Sportelli, L. *J. Magn. Reson.* **2003**, *162*, 371–379.
- (42) Ge, M.; Freed, J. H. *Biophys. J.* **1999**, *76*, 264–280.
- (43) Dzikovski, B. G.; Borbat, P. P.; Freed, J. H. *Biophys. J.* **2004**, *87*, 3504–3517.
- (44) Schweiger, A.; Jeschke, G. *Principles of Pulse Electron Paramagnetic Resonance*; Oxford University Press: Oxford, U.K., 2001; pp 208–229.
- (45) Sato, H.; Kathirvelu, V.; Spagnol, G.; Rajca, S.; Rajca, A.; Eaton, S. S.; Eaton, G. R. *J. Phys. Chem. B* **2008**, *112*, 2818–2828.
- (46) Zecevic, A.; Eaton, G. R.; Eaton, S. S.; Lindgren, M. *Mol. Phys.* **1998**, *95*, 1255–1263.
- (47) Volkov, A.; Dockter, C.; Bund, T.; Paulsen, H.; Jeschke, G. *Biophys. J.* **2009**, *96*, 1124–1141.

(48) Jeschke, G.; Panek, G.; Godt, A.; Bender, A.; Paulsen, H. *Appl. Magn. Reson.* **2004**, *26*, 223–244.

(49) Milov, A. D.; Samoilova, R. I.; Tsvetkov, Y. D.; Formaggio, F.; Toniolo, C.; Raap, J. *Appl. Magn. Reson.* **2005**, *29*, 703–716.

(50) Milov, A. D.; Erilov, D. A.; Salnikov, E. S.; Tsvetkov, Y. D.; Formaggio, F.; Toniolo, C.; Raap, J. *Phys. Chem. Chem. Phys.* **2005**, *7*, 1794–1799.

(51) Ollila, S.; Hyvönen, M. T.; Vattulainen, I. *J. Phys. Chem. B* **2007**, *111*, 3139–3150.

(52) Vogel, A.; Scheidt, H. A.; Huster, D. *Biophys. J.* **2003**, *85*, 1691–1701.

(53) Garay, A. S.; Rodrigues, D. E. *J. Phys. Chem. B* **2008**, *112*, 1657–1670.

(54) van den Brink-van der Laan, E.; Killian, J. A.; de Kruijff, B. *Biochim. Biophys. Acta* **2004**, *1666*, 275–288.

JP1060039